



## Testing the Origin of High Energy Cosmic Rays

TROY A. PORTER<sup>1</sup>, ANDREY E. VLADIMIROV<sup>1</sup>, IGOR V. MOSKALENKO<sup>1</sup>, GUDLAUGUR JÓHANNESSON<sup>2</sup>

<sup>1</sup> *W. W. Hansen Experimental Physics Laboratory, Stanford University, Stanford, CA 94305, USA*

<sup>2</sup> *Science Institute, University of Iceland, Dunhaga 5, IS-107 Reykjavík, Iceland*

*tporter@stanford.edu*

DOI: 10.7529/ICRC2011/V06/1201

**Abstract:** Recent accurate measurements of the cosmic-ray (CR) proton, helium, and heavier nuclei by ATIC-2, CREAM, and PAMELA reveal: a) unexpected hardening in the spectra of CR species above a few hundred GeV per nucleon, b) a harder spectrum of He compared to protons, and c) softening of CR spectra just below the break energy (a “dip”). These features may offer a clue to the origin of the observed high-energy Galactic CRs. We discuss possible interpretations of these spectral features and make predictions of the diffuse Galactic  $\gamma$ -ray emission, CR isotopic ratios, and anisotropy of CRs for different scenarios. Our predictions can be tested by currently running or near-future high-energy astrophysics experiments.

**Keywords:** astroparticle physics — diffusion — cosmic rays — ISM: general — diffuse radiation — gamma rays: ISM

## 1 Introduction

The data recently collected by ATIC-2 [1, 2], CREAM [3, 4], and PAMELA [5] indicate a break (hardening) of the spectra of the most abundant CR species above a rigidity of a few hundred GV. The break rigidity,  $\rho_{\text{br}}$ , is best measured by PAMELA occurring at approximately the same rigidity for protons and He,  $\rho_{\text{br}} \approx 240$  GV. The PAMELA data for  $\rho < \rho_{\text{br}}$  are in an excellent agreement with earlier data of AMS and BESS (see [6, 7] and Figure 1 of [5]). ATIC-2 data points for  $\rho < \rho_{\text{br}}$  are somewhat lower. Above the break,  $\rho > \rho_{\text{br}}$ , ATIC-2 results agree well with those of CREAM. From these data, we estimate the difference between the spectral indices below and above the break to be  $\Delta_{\text{br}} = \gamma(> \rho_{\text{br}}) - \gamma(< \rho_{\text{br}}) = 0.15$  for both protons and He.

Another important feature of the CR spectra discovered by these experiments is the difference between the spectral indices of CR protons and He, which has been discussed for a long time (e.g., [8], and references therein), but the experimental uncertainties were considerable [9]. The new measurements by PAMELA confirm this difference to high statistical accuracy. The He spectrum is found to be harder than the proton spectrum below  $\sim 10^4$  GeV/nucleon. The difference between the proton and He spectral indices calculated by [5] using the PAMELA data is  $\Delta\gamma = 0.10$ , and it is approximately the same above and below the break  $\rho_{\text{br}}$ . Within the statistical and systematic uncertainties the measured p/He flux ratio appears to be a smooth function of rigidity, continuous at  $\rho_{\text{br}}$ . This shows that the difference

in the spectral slope of p and He persists into the ultra-relativistic regime.

There is also fine structure in the spectra that may provide additional information: the PAMELA spectrum has a spectral softening (“dip”) at the break rigidity, which is statistically significant at the 95% confidence level for the spectra as functions of particle rigidity, and 99.7% level for the same data in terms of kinetic energy per nucleon [5]. The softening is more pronounced in the spectrum of He.

Rather than proposing a detailed interpretation, in this paper we classify possible scenarios for the production of the observed spectral features and discuss required adjustments to the standard picture of CR propagation. The quantitative analysis is done using the GALPROP code (see [10] and the project web site<sup>1</sup>). We also propose observational tests of these scenarios.

## 2 Interpretations

The following general categories of models (i.e. scenarios) are considered for the origin of the observed spectral features, the break at  $\rho_{\text{br}}$  and the “dip” at  $\rho < \rho_{\text{br}}$ : (i) interstellar propagation effects, (ii) modification of CR injection spectrum at the sources, (iii) composite Galactic CR spectrum, (iv) effects of the local sources and/or local medium at low energies ( $\rho < \rho_{\text{br}}$ ), and (v) effects of the local sources and/or local medium at high energies ( $\rho > \rho_{\text{br}}$ ). We briefly describe these scenarios and their ra-

1. <http://galprop.stanford.edu/>

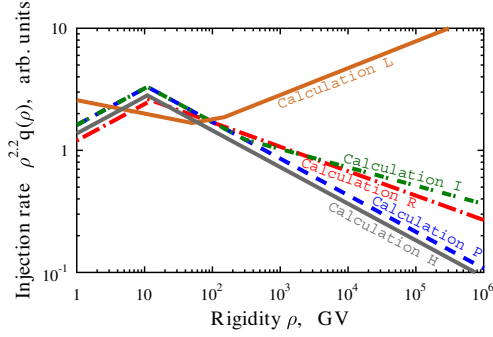


Figure 1: Galactic CR source injection spectrum in *Calculations R, P, I, L* and *H*. Units are arbitrary. The normalisation of the injection spectrum was chosen to obtain the best fit of proton and He spectrum at Earth. For all calculations, the lines represent the Galactic CR source injection spectrum. The local sources, present in *Calculation L* and *Calculation H*, are not shown here. The local source fluxes at Earth in *Calculation L* and *Calculation H* were obtained as the difference between the observed and the propagated Galactic fluxes.

tionale. Each *Scenario* is quantitatively analyzed with the respective *Calculation*.

*Scenario R: Reference scenario.* First, we introduce a reference scenario based on pre-PAMELA data. For this the CR injection spectrum above 10 GV is a single power law up to the “knee” around  $10^{15-16}$  eV, with the same index for all CR species, the diffusion coefficient has a uniform dependence on particle rigidity (i.e., without a break), and no local sources are assumed. *Calculation R* provides satisfactory agreement with pre-PAMELA data, but it cannot reproduce the new spectral features discussed in this paper: the spectral break, difference between proton and helium spectrum, or the “dip”.

*Scenario P: interstellar Propagation effects.* In this scenario, the break in the observed proton and He spectra is attributed to a change in CR transport properties at rigidity  $\rho_{\text{br}}$ . We represent this with *Calculation P*, which has a break in the rigidity dependence of  $D$  at  $\rho = \rho_{\text{br}}$ . For  $\rho < \rho_{\text{br}}$ , we use the functional form for  $D(\rho)$  obtained in the comprehensive analysis of CR data by [11], while for  $\rho > \rho_{\text{br}}$ , we adjust the rigidity dependence to match the observations of PAMELA, ATIC-2 and CREAM discussed above.

*Scenario I (a): cosmic ray Injection effects, source with a spectral break interpretation.* Some models of particle acceleration may predict a pronounced hardening in the spectrum of particles injected into the ISM, consistent with the new data. For example, in the model of [12], the break, or upturn, occurs due to the contribution of the remnant’s polar cap. This case, represented by *Calculation I*, features a Galaxy-wide source spectrum with a hardening at  $\rho_{\text{br}}$ . The diffusion coefficient does not have a break in this scenario.

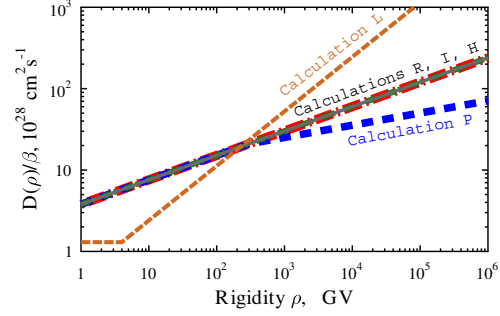


Figure 2: Diffusion coefficient of CRs in the Galaxy. The values of the  $D$  coincide for *Calculations R, I, L* and *H*. For *Calculation P*, a break in the diffusion coefficient is assumed, changing  $\delta_1/\delta_2 = 0.30/0.15$  at  $\rho_0 = 300$  GV.

*Scenario I (b): cosmic ray Injection effects, composite source interpretation.* While SNRs (isolated or in superbubble regions) are believed to be the primary source of Galactic CRs, different classes of supernovae and their environments, as well as other CR sources, can combine to produce the observed CR spectrum. If one Galactic source dominates the low energy part of the CR spectrum, and the other – the high energy part – then *Calculation I*, with a hardening of the Galactic CR source at  $\rho_{\text{br}}$ , includes this composite source scenario as well. We use the same computational setup to calculate the observed quantities for *Scenario I (a)* and *Scenario I (b)*, and we call it *Calculation I*. A subtle advantage of the composite source interpretation of *Calculation I* (i.e. in *Scenario I (b)*) is its ability to explain the “dip” more naturally than the source with an inherent break scenario.

*Scenario L: local Low energy source.* This scenario includes interpretations that assume that the observed spectral break is caused by a local source dominating the CR spectrum for rigidities below  $\rho_{\text{br}}$ . Unlike *Scenario I (b)*, this scenario assumes that the low-energy source is not typical for the Galaxy as a whole. This case is represented by *Calculation L*, where the Galactic CR spectrum is hard, fitting the observations of PAMELA, ATIC-2 and CREAM for  $\rho > \rho_{\text{br}}$ . For  $\rho < \rho_{\text{br}}$ , the flux of CRs from this source is lower than the observed flux, and we assume that the difference is accounted for by the hypothetical local source. We assume the extreme case of a very localised low energy source. This means that we do not calculate propagation of local source CRs throughout the Galaxy, and only the Galactic source is used to calculate the diffuse Galactic  $\gamma$ -ray emission. Note that *Scenario L* represents the extreme case of a very localised source, while *Scenario I (b)* is the opposite.

*Scenario H: local High energy source.* This case, represented by *Calculation H*, is analogous to *Scenario L*, but with the spectral break produced by a local high-energy source dominating the observed flux at  $\rho > \rho_{\text{br}}$ . The dif-

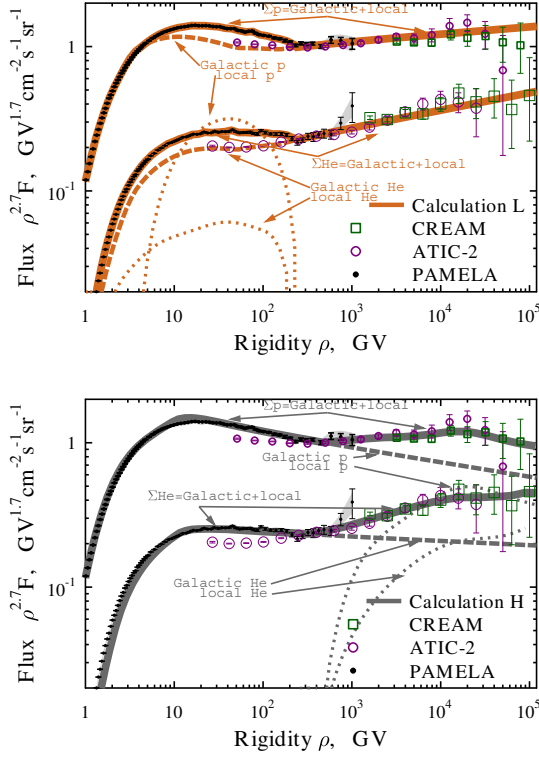


Figure 3: CR spectra in *Calculations H* and *L* and data of ATIC-2 [1, 2], CREAM [3, 4] and PAMELA [5].

fuse Galactic  $\gamma$ -ray emission is determined solely by the Galactic source, like in *Calculation L*.

### 3 Results and Discussion

For each scenario, we did the CR propagation calculations in the framework of the diffusive reacceleration model (except *Scenario L*), using the GALPROP code. Cosmic ray spectra were modulated using the “force-field” approximation [19] with a modulation potential  $\Phi = 450$  MV, appropriate for the solar activity level for the data used in this paper. Figures 1 and 2 show the corresponding source spectra and diffusion coefficients for each scenario. As an example of the propagation calculations, Fig. 3 shows the calculated p and He spectra for the *Calculation H* and *Calculation L* scenarios described above. These figures illustrate the different contributions to the CR spectra by the components for each of these models. Note, in the case of a local low-energy source scenario (i.e., *Scenario L*), the CR propagation model has been adjusted to account for the fresh component of low energy CRs.

Differences between scenarios could be reflected in the CR anisotropy, the B/C ratio at high energies (Fig. 7), antiproton flux and antiproton to proton ratio (Fig. 5), as well as the diffuse Galactic  $\gamma$ -ray emission (Fig. 6). The experi-

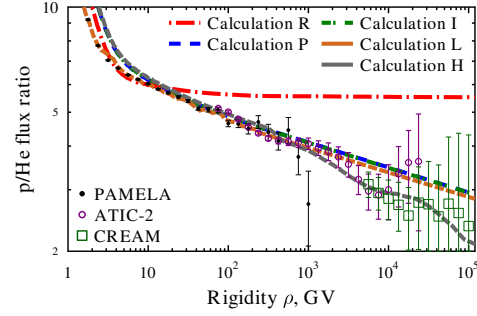


Figure 4: p/He ratio and data from ATIC-2 [1, 2], CREAM [3, 4] and PAMELA [5]

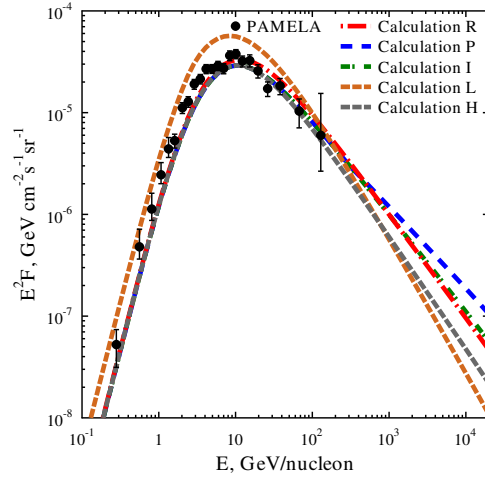


Figure 5: CR antiprotons: data of PAMELA [13] and calculation results.

mental uncertainty in the data does not allow any of the scenarios to be rigorously rejected. However, more accurate B/C data above  $10^2$  GeV/nucleon and  $\bar{p}$  data above 1 TeV may help to differentiate between these models. Note that for the  $\gamma$ -ray data, while the  $\pi^0$ -decay channel at 1 TeV differs in models with and without a hard high-energy CR tail, the *total*  $\gamma$ -ray flux, including the inverse Compton contribution, is virtually indistinguishable between the models.

The existing data does, however, allow some scenarios to be favoured based on phenomenological reasoning. Namely, the fact that p/He ratio at the break point is a continuous function of rigidity is naturally explained if the diffusive properties of the ISM are responsible for the break. However, if the break is the result of two different types of sources contributing to the CR spectrum, the above mentioned observation requires the same He/p ratio in both types of sources.

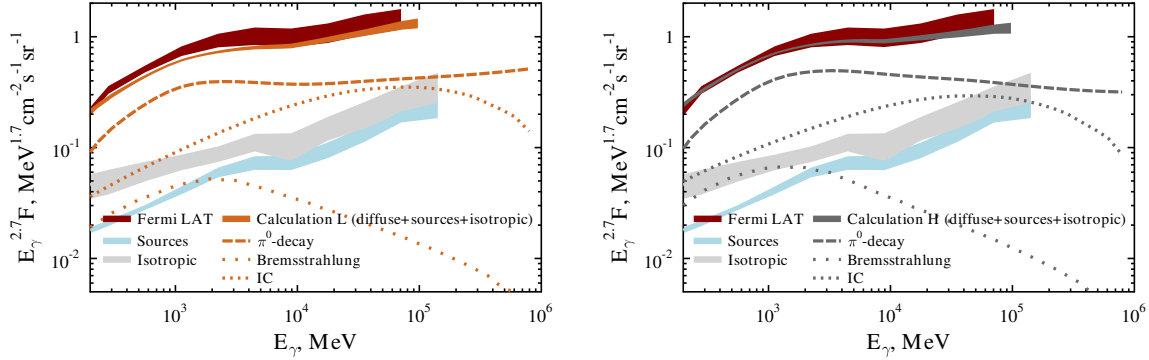


Figure 6: Diffuse  $\gamma$ -ray emission from intermediate Galactic latitudes. Calculation results and data from [14]. The data are averaged over intermediate Galactic latitudes  $10^\circ < |b| < 20^\circ$ , as reported in [14].

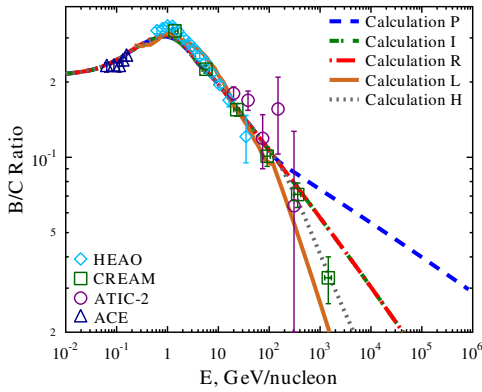


Figure 7: Boron/Carbon: data (ACE [15], HEAO-3 [16], CREAM [17] and ATIC-2 [18]) and calculation results.

One of the new features observed by PAMELA is the “dip” in proton and He spectra just below the break rigidity. The significance of this “dip” seems to be higher in the He spectrum. If confirmed, this “dip” poses a challenge for all considered scenarios except for *Scenario L*, where it may arise naturally if the spectrum of the local source has an exponential cutoff at the break energy.

Most specific physical models explaining p/He ratio, spectral break and the “dip” fall into one of the scenarios studied in this paper. We have demonstrated that only with data expected from current and future experiments such as *Fermi-LAT* and *AMS-2*, will it be possible to reject some of these scenarios and, along with them, advance our understanding of the origin of Galactic CRs.

## References

- [1] Wefel, J. P. et al. in International Cosmic Ray Conference, 2008, volume **2**, pages 31–34.
- [2] Panov, A. D. et al., Bulletin of the Russian Academy of Science, Phys., 2009, **73**, 564–567.
- [3] Ahn, H. S. et al., ApJ, 2010, **714**, L89–L93.
- [4] Yoon, Y. S. et al., ApJ, 2011, **728**(2), 122.
- [5] Adriani, O. et al., Science, 2011, **332**, 69–.
- [6] Alcaraz, J. et al., Phys. Lett. B, 2000, **490**, 27–35.
- [7] Haino, S. et al., Phys. Lett. B, 2004, **594**, 35–46.
- [8] Biermann, P. L., Gaisser, T. K., and Stanev, T., Phys. Rev. D, 1995, **51**, 3450–3454.
- [9] Moskalenko, I. V. et al., ApJ, 2002, **565**, 280.
- [10] Strong, A. W. and Moskalenko, I. V., ApJ, 1998, **509**, 212–228.
- [11] Trotta, R., Jóhannesson, G., Moskalenko, I. V., Porter, T. A., Ruiz de Austri, R., and Strong, A. W., ApJ, 2011, **729**, 106–+.
- [12] Biermann, P. L., Becker, J. K., Dreyer, J., Meli, A., Seo, E.-S., and Stanev, T., ApJ, 2010, **725**, 184–187.
- [13] Adriani, O. et al., Phys. Rev. Lett., 2010, **105**(12), 121101–+.
- [14] Abdo, A. A. et al., Phys. Rev. Lett., 2010, **104**(10), 101101–+.
- [15] Davis, A. J. et al. in Acceleration and Transport of Energetic Particles Observed in the Heliosphere, volume **528**, of American Institute of Physics Conference Series pages 421–424.
- [16] Engelmann, J. J., Ferrando, P., Soutoul, A., Goret, P., and Juliusson, E., A&A, 1990, **233**, 96–111.
- [17] Ahn, H. S. et al., APh, 2008, **30**, 133–141.
- [18] Panov, A. D. et al. in International Cosmic Ray Conference, 2008, volume **2**, pages 3–6.
- [19] Gleeson, L. J. and Axford, W. I., ApJ, 1968, **154**, 1011–+.